Advanced Materials
Manufacturing & Characterization

journal home page: www.ijammc-griet.com

Statistical Investigation into the Effects of Electro-Discharge Machining Parameters on WC/6%Co Composite-Part 1: Modeling through Response Surface Methodology (RSM)

S. Assarzadeh and M. Ghoreishi

Department of Mechanical Engineering, K. N. Toosi University of Technology, P.O. Box: 19395-1999, Tehran, Iran

ARTICLE INFO

Article history:
Received : 23-05-2013
Accepted : 29-07-2013

Keywords:
Analysis of variance (ANOVA),
Electro-discharge machining (EDM),
Face centered central (FCC) composite design,
Process modeling,
Response surface methodology (RSM),
Tungsten carbide cobalt composite (WC-Co).

ABSTRACT

In this two-part research, a unified approach is presented to model and optimize the electro-discharge machining (EDM) parameters on WC/6%Co using response surface methodology (RSM) and desirability function (DF) concept. In the first part, four controllable parameters, viz., discharge current (A), pulse on-time (B), duty cycle (C), and average gap voltage (D) have been selected as the input variables to evaluate the process performance in terms of material removal rate (MRR), tool wear rate (TWR), and arithmetic mean surface roughness (Ra) as the performance characteristics. The modeling phase begins applying face-centered central (FCC) composite design to plan and analyze the experiments in accordance with the RSM. For every response, the significant forms of influential parameters were properly identified conducting a comprehensive analysis of variance (ANOVA) at 1, 5, and 7% level of significance. It has been revealed that all the direct effects of input parameters are extremely momentous affecting both the MRR and TWR. Moreover, the pure quadratic effect of duty cycle (C^2), the reciprocal effects of discharge current with pulse on-time (A×B), duty cycle (A×C), and gap voltage (A×D), as well as the interaction amongst the pulse on-time with duty cycle (B×C) were also reached to be important terms affecting the MRR. The TWR measure behaves the same way, however, it exhibits a more nonlinear mathematical form containing the second order effect of discharge current (A^2) as an additional important term. On the other hand, for the Ra, the only significant parameters are the main effects of the first two inputs (A and B) plus the interactions of current with pulse on-time (A×B) and with gap voltage (A×D). The results indicate that the suitably proposed step-by-step implemented approach can substantially elucidate the highly multifaceted behavior of the chosen grade WC-Co under different EDM conditions providing a reliable platform to both navigating the operational region and seeking for optimal working circumstances confidently.

1. Introduction

Electro-discharge machining (EDM) is an electro-thermal erosion process where material is removed by a successive trend of controlled rapid and repetitive discrete electrical discharges (sparks), produced by a DC pulse generator, taking place between tool and work piece electrode submerged in a liquid dielectric medium [1-3]. It is the most popular non-traditional machining method capable of eroding every electrically conductive material with an electrical resistivity threshold value of the order between 100-300 Ωcm as the only limiting factor to support sparking [4]. Since thermo-electric energy is used instead of mechanical forces, work-based metallurgical and micro structural properties such as strength, hardness, toughness, etc have no barrier against its applicability. For decades, the process has gained considerably popular applications in machining various engineering materials, especially high-strength, temperature-resistant (HSTR) alloys (Inconel, Titanium, Beryllium alloys) [5-7], hard composites (metal matrix composites, nano-composites) [8, 9], conductive ceramics [4, 10], etc. in miscellaneous industries, mostly, aeronautic, die, mould, and automobile industries, with the additional versatility as being a very promising approach towards micro- as well as nano-machining technologies [11, 12].

Tungsten carbide-cobalt composite, amongst the most widely used difficult-to-cut materials, is one of the most important engineering materials with extreme applications in

- Corresponding author: M. Ghoreishi
- E-mail address: ghoreishi@kntu.ac.ir

- Doi: http://dx.doi.org/10.11127/ijammc.2013.07.03

manufacturing carbide dies and molds, cutting tools, forestry tools, and components resisting continual wear in production lines [13]. Its acutely high hardness and strength along with superior wear and corrosion resistance over a wide range of temperature has frustrated conventional machining processes of being utilized efficiently in shaping such a material. Just pendulum grinding with the help of special and expensive disks [14] and turning with cubic boron nitride (CBN) tools [15] were reported as the only feasible traditional machining methods applied in shaping and cutting WC-Co composites. Nevertheless, the results have shown limited success due to very low material removal rates, excessive tool wear, and high cost of tooling and production. Though, the EDM process has now been recognized and justified as the best and perhaps the only proficient machining candidate for cutting and shaping tungsten carbides, however, the process is not an easy going task [16]. Furthermore, unlike steel, often chosen as a general option for work piece material in EDM applications, it has been postulated that the behavior of ceramic composites, such as WC-Co, can be rather different in response to various parameters under the EDM process [4, 10, 17] which still needs to be further studied as cited by Garg et al. [18]. The main difficulty in EDMing WC-Co originates from its non-homogeneous structure, the differences between melting and evaporation points of the two constituent phases present in its micro-structure, i.e., WC and Co grains which may cause non-uniformity in erosion as well as process instability, producing short circuits and arcing pulses more frequently [16]. The melting and vaporization points of WC are about 28000C and 60000C, respectively, and those for Co are about 13200C and 27000C, both at normal atmospheric pressure [16]. Hence, during the EDM, the cobalt matrix first starts being removed from the surface by melting and evaporation mechanisms due to sparking. This early selective decomposition of WC-Co structure will lead to dislodging coarse WC grains into the gap space increasing the risk for process instability as a result of high debris accumulation and pollution inside gap region. Moreover, there is a noticeable difference in thermal expansion coefficients of WC and Co, the latter possessing a much higher one (14×10^{-6} 1/0C for Co as compared to 5×10^{-6} 1/0C for WC) [10, 16]. The discrepancy is responsible for developing high thermal tension stresses during re-solidification and quenching, exceeding the fracture strength of the material in the crater, and thus, causing abundance of cracks on the surface layer. For these reasons, the electro discharge machining of WC-Co composite is regarded as a challenging task imposing more difficulties compared to EDMing different kinds of hardened steels commonly studied in research articles.

2. Experimental specifics

2.1. Machine tool, tool electrode, work piece and dielectric materials

Azarakhsh ZNC spark erosion machine, model number 204 has been used to run the experiments. Equipped with an iso-frequency pulse generator, it can produce pulse-on times in the range 2µs-1000µs and provide maximum discharge current up to 75 A. Tungsten carbide cobalt composite, type WMG10, manufactured by Wolframcarb Company, Italy, available in cylindrical form (Φ12mm × 300 mm) has been selected as work piece material. A Charmilles Robofil 290 WEDM machine has been used to cut the blanks into 10 mm height to collect experimental samples. The selected WC-Co composite, produced via powder metallurgy, having about 94%wt WC and 6%wt Co as nominal chemical composition, is of a fine grain type and mainly used in fabricating drawing dies, woodworking tools as well as cutting tools for non-ferrous metals. Table 1 lists the relevant work piece material properties while Figure 1 illustrates its SEM micrograph.

As for the tool electrode material, electrolytic copper rods with the same diameter as work piece were used. The physical and mechanical properties are a density of 8.9 g/cm3, thermal conductivity 226 W/mK, electrical resistivity 9 µΩcm, melting point 1083 0C, and hardness about 100 HB. Copper has the additional advantageous as being easily available, stable in quality and cheap compared to other applicable metals. Thereupon, the EDM experiments were all conducted in planing mode in which both the tool and work piece bottom surfaces were ground prior to experimentation to remove any possible machining marks or irregularities assuring consistent gap width and flushing action. Moreover, commercial grade kerosene ejected as impulse side flushing through a nozzle was used as dielectric. Also, tool and work piece electrode polarity were assigned as positive and negative, respectively, as this status can make tool wear minimum along with stable sparking [10].

Table 1. Work piece thermo-physical and mechanical properties

Material composition	WC-6%wtCo (Iso grade: K10)
Hardness (HRA)	92.5
Melting point (^{0}C)	2870
Boiling point	6000^{0}C
Density (g/cm^3)	14.3
Transverse strength (MPa)	1700
Compressive strength (MPa)	6200
Modulus of Elasticity (GPa)	620
Thermal conductivity (Wm^{-1}K^{-1})	79.6
Thermal expansion coefficient (1/^{0}C)	5.5×10^{-6}

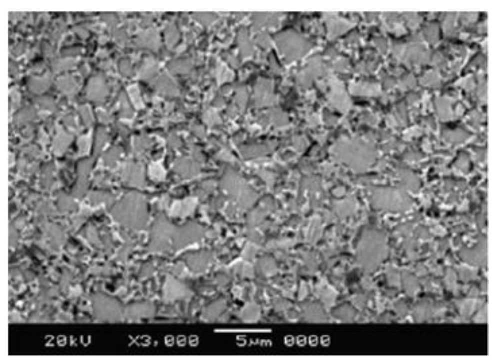

Figure 1. SEM image of the as-produced WC-6%Co composite

2.2. Machining parameters, design of experiments, and measurements

Four controllable input variables, namely, discharge current (A: Amp), pulse-on time (B: µs), duty cycle (C: %), and average gap (reference) voltage (D: Volt) have been selected as the predominant factors based on the EDM machine operating characteristics and consulting respective bibliography. These factors are the most relevant electrical-based parameters governing the discharge energy which is the most responsible item in EDM process efficiency [1, 2].

Face-centered central composite design (CCD) [19-21], a popular variant of central composite design of experiments, has been employed to plan the experiments. It is a kind of second order design class which uses three levels for each parameter and can efficiently handle linear, quadratic as well as interaction terms in process modeling. Generally, to collect enough data establishing a suitable second order regression response equation for a process involving k variables, the following three sets of design points are needed:

(a) $n_f = 2^k$ factorial design or corner points

(b) $n_a = 2k$ axial or star points, and

(c) n_c center points, which are usually repeated several times to obtain a good estimation of experimental pure error.

Then, the total number of experiments would be:

$$N = n_f + n_a + n_c = 2^k+2k + n_c \tag{1}$$

The location of axial points in a response surface central composite design with respect to the center point (origin) is determined by alpha (α) value. The choice of α depends to a great extent on the domain of operation and interest [19]. In face-centered central composite design, α = 1, meaning that a three-level design space, coded as -1, 0, and 1 corresponding to low, medium, and high parameter level, respectively. To specify the actual levels of each input variable, at first, a number of preliminary tests were conducted as one-factor-at-a-time (OFAT) approach to determine the most stable combination of parameter settings over the operability region of EDM machine [22]. Table 2 summarizes the relevant machining conditions and fixed parameters whereas Table 3 lists the preferred input controllable parameters along with their considered ranges in both coded and actual format.

Table 2. The EDM conditions

Working condition	Description
Workpiece material	WC-6%Co
Tool material	Commercial electrolytic copper
Polarity	Workpiece (-), tool (+)
Tool and workpiece dimensions	Cylindrical, Φ 12 mm
Peak current	2-8 A
Pulse-on time	50-150 µs
Duty cycle	40-80 %
Gap voltage	40-80 V
Dielectric fluid	Commercial kerosene
Dielectric flow rate	5 L/min
Flushing pressure/type	1 MPa/side flushing
ED-Machining time	60-90 min

Table 3. Selected input factors and levels for the face-centered CCD

Parameter	Notation	Unit	Coded/Actual level		
			-1	**0**	**+1**
Discharge current (I)	A	Ampere	2	5	8
Pulse on-time (T_{on})	B	µs	50	100	150
Duty cycle (DC)	C	-	40	60	80
Gap voltage (V)	D	Volt	40	60	80

Note: Duty cycle = pulse on-time/(pulse on-time + pulse off-time)

The response variables were then chosen as material removal rate (MRR: g/h), tool wear rate (TWR: g/h), and average surface roughness (Ra: µm). Both the stock removal rate and tool wear rate were measured directly by weight loss method, weighing work piece and tool electrode samples before and after each test and dividing the corresponding weight difference by the elapsed time allocated for each experimental run. A GX-200 digital single pan balance, manufactured by A&D Company, Japan, with a precision of 0.001 g and maximum capacity of 210 g has been used for the evaluation. During running the first round experiments, it was revealed that much longer times were needed to get a reasonable idea about the MRR as the removal efficiency for cemented carbides are very small compared to steels due to its extremely hardness and wear resistance [22]. So, the time allocated to each trial was at least an hour and much longer times were considered for runs with lower discharge currents. Characterization of each work piece surface condition was conducted in term of arithmetic mean deviations of roughness profile from the central line along the measurement path. Mahr-PS1 unit, a portable stylus type profilemeter made-up by Mahr Company, Germany, was used for roughness assessments. Before measuring surface roughness, each machined sample was cleaned in acetone liquid and dried with cold air blower. To achieve validity and accuracy, each Ra measurement was repeated two times along two different directions, as there is no specific pattern for spark distribution over the work area. The average of the two replications was then assigned as the roughness value for each treatment combination. Figure 2 shows a picture of the measuring device. In all cases, a cutoff length of 0.8 mm and an evaluation length of 4 mm (5×0.8 mm) were adjusted on the unit according to ISO 4287/1.

Figure 2. Mahr-PS1 surface roughness measuring unit

By repeating seven center points, the total numbers of conducted experiments for k = 4 was 24+2(4) + 7 = 31, and are shown in Table 4 along with the corresponding process responses. Figure 3(a) and (b) depicts two typical roughness profiles equivalent to two extreme cases, Exp. No. 19 and Exp. No. 16 in Table 4, processed by the MarSurf PS1 Explorer software, version 1.00-10, having the lowest and highest value of Ra, respectively.

The linear relationship between coded and actual values, in Tables 3 and 4 is as follow:

Discharge current: $A = [I-(I_{max}+I_{min})/2]/ (I_{max}-I_{min})/2$

Pulse on-time: $B = [T_{on}-(T_{onmax}+T_{onmin})/2]/ (T_{onmax}-T_{onmin})/2$

Duty cycle: $C = [DC-(DC_{max}+DC_{min})/2]/ (DC_{max}-DC_{min})/2$

Gap voltage: $D = [V-(V_{max}+V_{min})/2]/ (V_{max}-V_{min})/2$

where A, B, C, and D are the coded values of variables I, T_{on}, DC, and V, respectively, I_{max}, T_{onmax}, DC_{max}, and V_{max} respresent the maximum values of I, T_{on}, DC, and V, respectively, and, I_{min}, T_{onmin}, DC_{min}, and V_{min} are the corresponding minimum values of process parameters in each interval.

Finally, it is to be noted that the order of experimentation was randomized according to the second column of Table 4 (run number) to avoid creeping the effect of any possible extraneous or nuisance factor into the results [19].

Table 4. Design layout and experimental results

Exp. No.	Run No.	Input process parameters								Response variables				
		Coded				Actual				MRR (g/h)	TWR (g/h)	Ra_1 (µm)	Ra_2 (µm)	Ave. Ra (µm)
		A	B	C	D	I (A)	T_{on} (µs)	D.C. (%)	V (V)					
1	4	-1	-1	-1	-1	2	50	40	40	0.067	0.013	4.203	4.182	4.193
2	24	1	-1	-1	-1	8	50	40	40	0.54	0.09	3.533	3.689	3.611
3	10	-1	1	-1	-1	2	150	40	40	0.04	0.007	5.280	5.169	5.225
4	30	1	1	-1	-1	8	150	40	40	0.26	0.05	5.395	5.988	5.692
5	7	-1	-1	1	-1	2	50	80	40	0.153	0.027	3.673	3.508	3.591
6	28	1	-1	1	-1	8	50	80	40	0.86	0.15	4.292	4.606	4.048
7	15	-1	1	1	-1	2	150	80	40	0.097	0.014	5.149	5.449	5.299
8	1	1	1	1	-1	8	150	80	40	0.62	0.1	5.670	5.935	5.803
9	20	-1	-1	-1	1	2	50	40	80	0.02	0.013	3.712	3.769	3.741
10	11	1	-1	-1	1	8	50	40	80	0.12	0.04	4.203	4.286	4.245
11	27	-1	1	-1	1	2	150	40	80	0.04	0.007	4.488	4.404	4.446
12	8	1	1	-1	1	8	150	40	80	0.2	0.04	6.159	6.563	6.361
13	23	-1	-1	1	1	2	50	80	80	0.147	0.027	3.642	3.649	3.646
14	12	1	-1	1	1	8	50	80	80	0.672	0.132	4.424	4.633	4.529
15	6	-1	1	1	1	2	150	80	80	0.067	0.007	4.777	4.790	4.784
16	26	1	1	1	1	8	150	80	80	0.44	0.09	6.907	6.271	6.589
17	18	-1	0	0	0	2	100	60	60	0.080	0.02	5.154	5.362	5.258
18	2	1	0	0	0	8	100	60	60	0.48	0.09	4.713	4.766	4.740
19	22	0	-1	0	0	5	50	60	60	0.368	0.064	3.329	3.461	3.395
20	14	0	1	0	0	5	150	60	60	0.216	0.032	5.902	6.014	5.958
21	5	0	0	-1	0	5	100	40	60	0.152	0.024	5.630	5.368	5.499
22	29	0	0	1	0	5	100	80	60	0.36	0.048	4.254	4.817	4.536
23	17	0	0	0	-1	5	100	60	40	0.344	0.056	4.632	4.726	4.679
24	25	0	0	0	1	5	100	60	80	0.232	0.04	5.056	5.278	5.167
25	9	0	0	0	0	5	100	60	60	0.272	0.04	5.645	5.448	5.547
26	21	0	0	0	0	5	100	60	60	0.280	0.048	4.658	4.519	4.589
27	13	0	0	0	0	5	100	60	60	0.296	0.048	4.675	4.632	4.654
28	31	0	0	0	0	5	100	60	60	0.288	0.04	5.177	5.283	5.230
29	16	0	0	0	0	5	100	60	60	0.272	0.04	4.840	4.557	4.699
30	19	0	0	0	0	5	100	60	60	0.264	0.048	4.821	5.153	4.987
31	3	0	0	0	0	5	100	60	60	0.272	0.048	5.632	5.495	5.564

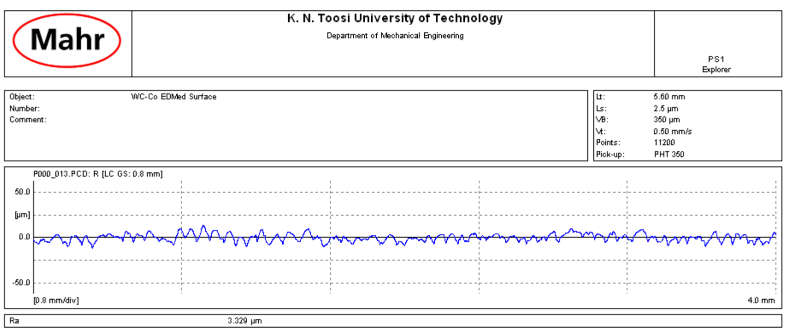

(a)

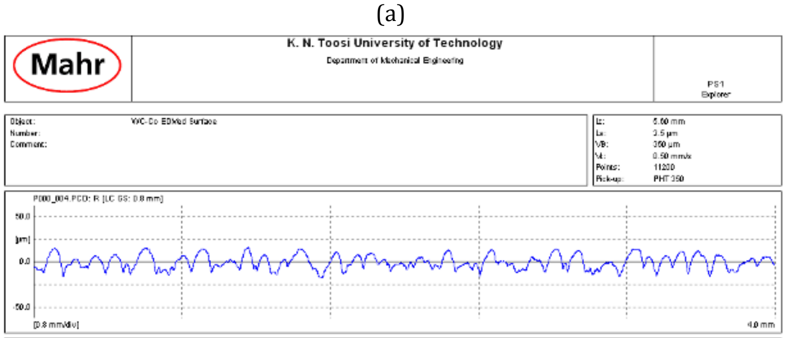

(b)

Figure 3. Surface roughness profiles for the two extreme conditions equivalent to (a) minimum Ra: Exp. No. 19, and (b) maximum Ra: Exp. No. 16 as per Table 4.

3. Response surface modeling of process measures

The practical optimization of EDM parameters on WC-Co composite necessitates accurate model building of the process responses describing its behavior and characteristics under different operating conditions. Response surface methodology (RSM) [19-21], a collection of mathematical and statistical techniques aimed at developing suitable second order polynomial models by multiple linear regression analysis, has been employed here. The model, in terms of the observations, in matrix notation is:

$$\boldsymbol{y} = \boldsymbol{X\beta} + \boldsymbol{\varepsilon} \tag{2}$$

where $\boldsymbol{y}$ is a (n×1) vector of observations (n is the number of observations), $\boldsymbol{X}$ is an (n×p) matrix of the levels of the independent variables (p = k+1, k is the number of process variables or regressors), $\boldsymbol{\beta}$ is a (p×1) vector of the regression coefficients and $\boldsymbol{\varepsilon}$ is an (n×1) vector of random errors. The vector of fitted values $\hat{y}_i$ corresponding to the observed values y_i (fitted regression model) is then [20]:

$$\hat{\boldsymbol{y}} = \boldsymbol{X}\hat{\boldsymbol{\beta}} \tag{3}$$

where $\hat{\boldsymbol{\beta}}$ is the least squares estimators of regression coefficients ($\boldsymbol{\beta}$), $[\beta_0, \beta_1, \beta_2, \dots, \beta_k]^T$, and can be calculated based on the following equation:

$$\hat{\boldsymbol{\beta}} = (\boldsymbol{X}'\boldsymbol{X})^{-1}\boldsymbol{X}'\boldsymbol{y} \tag{4}$$

In the above equation, $\boldsymbol{X}'$ is the transpose of matrix $\boldsymbol{X}$, $\boldsymbol{X}'\boldsymbol{X}$ is a (p×p) symmetric matrix and $\boldsymbol{X}'\boldsymbol{y}$ is a (p×1) column vector. Therefore,

$$\hat{\boldsymbol{y}} = \boldsymbol{X}\hat{\boldsymbol{\beta}} = \boldsymbol{X}(\boldsymbol{X}'\boldsymbol{X})^{-1}\boldsymbol{X}'\boldsymbol{y} = \boldsymbol{H}\boldsymbol{y} \tag{5}$$

The n×n matrix $\boldsymbol{H} = \boldsymbol{X}(\boldsymbol{X}'\boldsymbol{X})^{-1}\boldsymbol{X}'$ is usually called the hat matrix playing a central role in regression analysis and maping the vector of observed values into a vector of fitted values. The difference between the actual observed value y_i and the corresponding fitted value $\hat{y}_i$ is the residual, $e_i = y_i - \hat{y}_i$, a (n×1) vector. The *n* residuals may be conveniently written in matrix notation as

$$\boldsymbol{e} = \boldsymbol{y} - \hat{\boldsymbol{y}} = \boldsymbol{y} - \boldsymbol{X}\hat{\boldsymbol{\beta}} = \boldsymbol{y} - \boldsymbol{H}\boldsymbol{y} = (\boldsymbol{I} - \boldsymbol{H})\boldsymbol{y} \tag{6}$$

where $\boldsymbol{I}$ is an (n×n) identity matrix. In scalar notation, the general form of a fitted response surface quadratic model can be written as:

$$\hat{y} = \beta_0 + \sum_{i=1}^{k}\beta_i x_i + \sum_{i=1}^{k}\beta_{ii} x_i^2 + \sum_{i=1}^{k-1}\sum_{j=i+1}^{k}\beta_{ij} x_i x_j \tag{7}$$

The intercept coefficient β_0 represents the response at the center of the experiments where all the variables are zero (in coded form); β_i, β_{ii}, and β_{ij} also show the linear, quadratic, and linear-by-linear interaction effects of the parameters, respectively. This second-order polynomial is the most commonly used form and works quite well for a relatively small region of the variable space. Applying the least squares method (LSM) [19-21], all these coefficients in a multiple regression model can be estimated.

In this study, the quantitative form of relationship between desired responses and independent input variables can be represented by the following form:

$$y = f(I, T_{on}, DC, V) \tag{8}$$

where y is the desired response and f is the response function or surface. The steps consisting applying regression analysis, performing pooled ANOVA on each obtained regression coefficients to find statistically significant terms, and finally conducting ANOVA and some routine statistics to check modeling adequacy and goodness of fit are the necessary actions needed to be carefully executed to find the suitable reduced quadratic forms of response functions, MRR, TWR, and Ra for the highly stochastic process of EDM on WC-6%Co. The next sections focus on these procedures.

4. Results and discussion

4.1. Response surface modeling of MRR, TWR, and Ra

Based on the model described by Eq. (7) and by applying the LSM, all the regression coefficients pertaining to the three responses have been obtained and are shown in Table 5 along with their corresponding Student T- and P-values as a pooled ANOVA format. As is clear from this Table, all the main effects of four input parameters (A: discharge current, B: pulse on-time, C: duty cycle, and D: gap voltage) are found to be highly significant at least at a α = 0.01 significance level or 99% confidence interval, having almost zero P-values in affecting both the MRR and TWR. However, for the third response, Ra, just the first two factors, discharge current (A) and pulse-on time (B) are regarded as the highly significant main factors. In the terminology of statistical modeling, the lower the P-value, the more influential is the effect [19-21]. Additionally, the pure quadratic effect of duty cycle (C^2), the two-way interactions of discharge current with pulse-on time (A×B), with duty cycle (A×C), and with gap voltage (A×D), as well as the interaction amongst the pulse on-time with duty cycle (B×C) were also found to be extremely important terms influencing the MRR. For the TWR measure, the second order effect of discharge current (A^2) was also known to be significant term in addition to the aforementioned ones for the MRR conveying a more nonlinear mathematical form. Finally, for the Ra quality measure, the only considerable interactive terms are discharge current with pulse-on time (A×B) and with gap voltage (A×D). As a whole, the inclusion of any term with a P-value less than 0.07 designated as an upper bound for statistical significance; i.e., being significant within 93% of confidence interval, has been guaranteed in this research so as to increase each model's accuracy and sufficiency as high as possible. All the other terms not meeting such a criterion are supposed to be insignificant. Generally, the term "*interaction*" means that the effect of a factor over a known response depends on the level of another factor. Identifying significant interaction terms in RSM model building procedure and their inclusions in the structure of a second order model are of vital importance as they can reveal very crucial phenomena of the combinatorial joint effects of different process parameters on every process characteristics and behavior [19-21]. Removing insignificant terms is a common practice amongst empirical model builders which, in most cases, can result in improved model fitting capabilities aside from yielding simpler model form. Thereupon, the insignificant terms have been excluded from the models' structures through backward elimination method [19-21] and the ANOVA has been repeated for every obtained reduced quadratic model containing only those significant terms contributing to model building. The results are illustrated in Table 6.

As are desired, all the quadratic regression models are significant while their lacks of fits were turned out to be insignificant relative to pure error. Hence, the model adequacy checking is completely assured for each output measure. Other statistical diagnostic indices mainly used to evaluate the modeling goodness of fit are the ordinary R-squared (R^2), adjusted R-squared (R^2_{Adj}), and predicted R-squared (R^2_{Pred}) [20], shown inside Table 6 for every response model. The values are 99.74%, 99.59%, and 98.51% for MRR; 97.58%, 96.38%, and 91.13% for TWR; and 80.93%, 77.12%, and 74.1% for Ra, respectively. As a general rule, the more the R^2s approach unity, the better the model fits the experimental data [19-21]. The usual statistic R^2, also called the coefficient of multiple determination, indicates how many percent of the total variations can be explained by the model while the R^2_{Adj}, a statistic adjusted for the size (the number of factors) of model, means how many percent of the total variability can be explained by the model after considering the significant terms (reduced model). The amount of R^2 increases as each additional variable or regressor, whether significant or insignificant, is added to the model. On the contrary, the adjusted R^2 does not automatically increase when new predictor variables are added to the model. In fact, the value of adjusted R^2 will often decrease when unnecessary terms are included. Accordingly, when R^2 and R^2_{Adj} differ dramatically, there is a good chance that insignificant terms have been incorporated in the model [19-21]. Therefore, it is a suitable criterion in evaluating a model's goodness of fit when only significant terms are involved compared to the case when all the terms are caught up. The statistic PRESS (prediction error sum of squares) is a measure of how well the model will predict new data. A model with a small value of PRESS is desired as it indicates that the model is likely to be a good predictor [20]. In connection with this, the predicted R^2 (R^2_{Pred}) is defined which is an indication of the predictive capability of regression model in response to new observations.

The R^2s coefficients and PRESS statistic are calculated as [19-21]:

$$R^2 = \frac{SS_R}{SS_T} = 1 - \frac{SS_{Res}}{SS_T} \tag{9}$$

$$R_{Adj}{}^2 = 1 - \frac{SS_{Res}/(n-p)}{SS_T/(n-1)} = 1 - \frac{MS_{Res}}{MS_T} = 1 - \left(\frac{n-1}{n-p}\right)(1-R^2) \tag{10}$$

$$R_{Pred}{}^2 = 1 - \frac{PRESS}{SS_T} \tag{11}$$

$$PRESS = \sum_{i=1}^{n} e_{(i)}{}^2 = \sum_{i=1}^{n} \left[y_i - \widehat{y_{(i)}}\right]^2 \tag{12}$$

where, SS_R is the regression sum of squares, SS_T is the total sum of squares, SS_{Res} is the residual sum of squares, MS_{Res} is the residual mean square, MS_T is the total mean square, and $\widehat{y_{(i)}}$ is the predicted value of the ith observed response based on a model fit to the remaining (n-1) sample points. More details can be found in [19-21]. A broad overview of these indices confirms suitability and completeness of all the obtained models as neither inconsistency nor poor adequacy can be observed.

A complete residual analysis has also been done for every developed response and the graphs are shown in Figure 4 (A-C). Normal probability plot of residuals reveals that experimental data are spread approximately along a straight line, confirming a good correlation between experimental and predicted values for the response (Figure 4, A(a), B(a), and C(a)). In graph of residuals versus fitted values (Figure 4, A(b), B(b), and C(b)), only small variations can be seen. The histogram of residuals (Figure 4, A(c), B(c), and C(c)) also shows a Gaussian distribution which is desirable, and finally, in residuals against the order of experimentations in Figure 4, A(d), B(d), and C(d) both negative and positive residuals are apparent indicating no special trend which is worthy from statistical point of view. As a whole, all the yielded models do not show any inadequacy.

Table 5. Regression coefficients and T-test results for the individual MRR, TWR, and Ra model parameters

Predictor	MRR model			TWR model			Ra model		
	Coefficient	T-value	P-value	Coefficient	T-value	P-value	Coefficient	T-value	P-value
Constant	0.2790	80.939	<0.0001[a]	0.0449	22.803	<0.0001[a]	5.0082	38.649	<0.0001[a]
A	0.2003	34.796	<0.0001[a]	0.0359	22.957	<0.0001[a]	0.3019	2.933	0.010[a]
B	-0.0631	-17.705	<0.0001[a]	-0.0116	-7.416	<0.0001[a]	0.8421	8.179	<0.0001[a]
C	0.1029	17.869	<0.0001[a]	0.01728	11.035	<0.0001[a]	-0.0104	-0.101	0.920
D	-0.0527	-14.787	<0.0001[a]	-0.0062	-3.939	0.001[a]	0.0759	0.738	0.471
A^2	-0.0004	-0.058	0.954	0.0096	2.337	0.033[b]	0.0263	0.097	0.924
B^2	0.0116	1.602	0.137	0.0026	0.640	0.531	-0.2962	-1.092	0.291
C^2	-0.0244	-3.379	0.006[a]	-0.0094	-2.270	0.037[b]	0.0448	0.165	0.871
D^2	0.0076	1.048	0.317	0.0026	0.640	0.531	-0.0497	-0.183	0.857
AB	-0.0375	-7.249	<0.0001[a]	-0.0054	-3.274	0.005[a]	0.2143	1.962	0.067[c]
AC	0.0718	10.074	<0.0001[a]	0.0136	8.167	<0.0001[a]	0.0841	0.770	0.453
AD	-0.0481	-9.306	<0.0001[a]	-0.0051	-3.048	0.008[a]	0.2663	2.439	0.027[b]
BC	-0.0207	-4.002	0.002[a]	-0.0046	-2.747	0.014[b]	0.0454	0.416	0.683
BD	0.0067	1.687	0.120	0.0026	1.543	0.142	-0.0348	-0.319	0.754
CD	0.0080	1.539	0.152	0.0016	0.941	0.361	0.0459	0.421	0.680

Note: [a] Significant at α = 1% significance level; [b] Significant at α = 5% significance level; [c] Significant at α = 7% significance level

Table 6. ANOVA table for the trimmed MRR, TWR, and Ra second order models

Source	DF	Seq SS	Adj MS	*F* value	*P* value	Remarks
(a) For MRR						
Regression	9	1.05761	0.11751	676.09	0.000	*Significant*
Linear	4	0.98063	0.22721	1307.20	0.000	
Square	1	0.00825	0.00066	3.79	0.069	
Interaction	4	0.06874	0.01718	98.86	0.000	
Residual error	16	0.00278	0.00017	-	-	
Lack-of-fit	10	0.00250	0.00021	1.68	0.271	*Insignificant*
Pure error	6	0.00073	0.00012	-	-	
Correlation Total	25	1.06039	-	-	-	
$R^2 = 99.74\%$ $R^2_{Adj} = 99.59\%$ $R^2_{Pred} = 98.51\%$ PRESS = 0.01577						
(b) For TWR						
Regression	10	0.03641	0.00364	80.76	0.000	*Significant*
Linear	4	0.03174	0.00794	176.02	0.000	
Square	2	0.00051	0.00025	5.64	0.011	
Interaction	4	0.00415	0.00104	23.07	0.000	
Residual error	20	0.00090	0.00005	-	-	
Lack-of-fit	14	0.00079	0.00006	3.09	0.086	*Insignificant*
Pure error	6	0.00011	0.00002	-	-	
Correlation Total	30	0.03731	-	-	-	-
$R^2 = 97.58\%$ $R^2_{Adj} = 96.38\%$ $R^2_{Pred} = 91.13\%$ PRESS = 0.00331						
(c) For Ra						
Regression	5	16.379	3.2758	21.22	0.000	*Significant*
Linear	3	14.510	4.8365	31.33	0.000	
Interaction	2	1.870	0.9348	6.06	0.007	
Residual error	25	3.859	0.1544	-	-	
Lack-of-fit	9	1.942	0.2158	1.80	0.146	*Insignificant*
Pure error	16	1.917	0.1198	-	-	
Correlation Total	30	20.239	-	-	-	
$R^2 = 80.93\%$ $R^2_{Adj} = 77.12\%$ $R^2_{Pred} = 74.10\%$ PRESS = 5.24248						

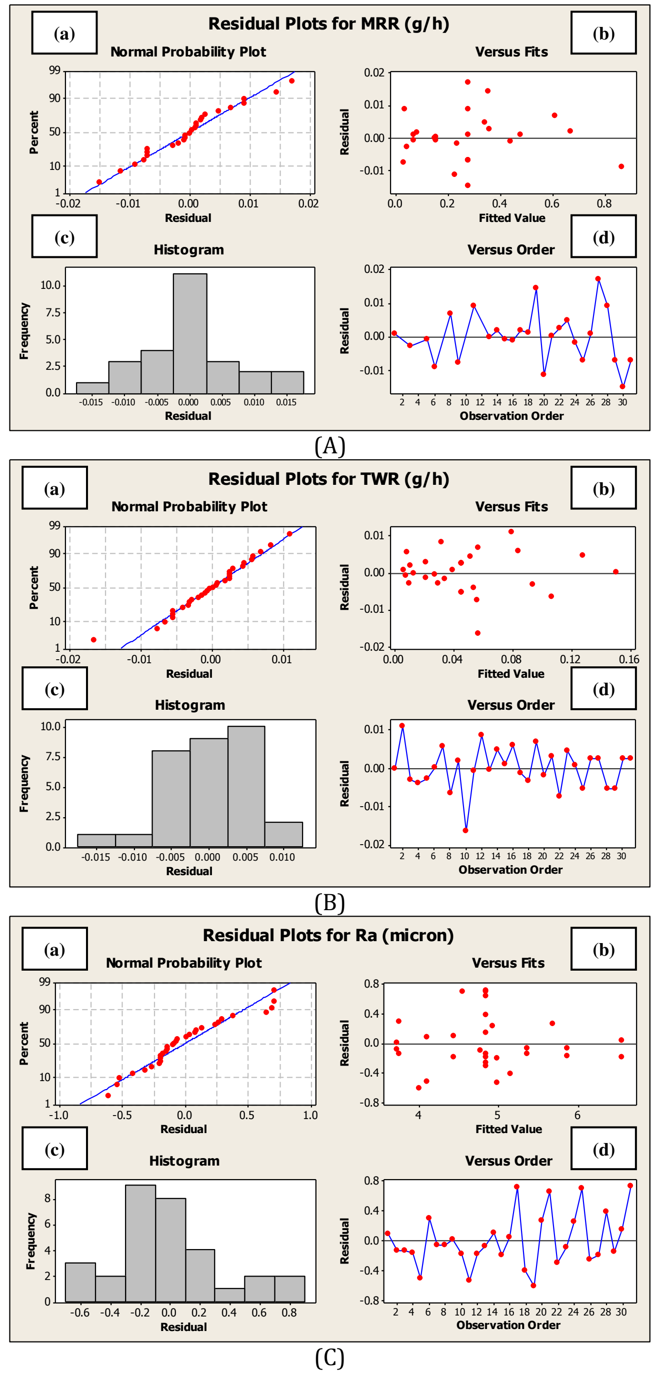

Figure 4. Plot of residuals: (A) MRR, (B) TWR, (C) Ra ((a) normal probability plot of residuals, (b) residuals versus the fitted values, (c) histogram of the residuals, and (d) residuals against the order of data)

Table 7 also details all the numerical values of finalized individual regression coefficients for every response. Based on these, the mathematical equations are conformed for each performance characteristics to suitable coefficients and can be expressed in terms of coded factors as:

$$MRR = 0.282 + 0.194A - 0.063B + 0.110C - 0.051D - 0.014C^2 - 0.041AB + 0.076AC - 0.042AD - 0.017BC \quad (13)$$

$$TWR = 0.045 + 0.036A - 0.012B + 0.017C - 0.006D + 0.012A^2 - 0.007C^2 - 0.005AB + 0.014AC - 0.005AD - 0.005BC \quad (14)$$

$$Ra = 4.849 + 0.302A + 0.842B + 0.076D + 0.214AB + 0.266AD \quad (15)$$

The above developed models can be used as reliable tools navigating the design space within the process parameters domain to get an in-depth understanding of process characteristics and can also be utilized in the optimization stage to find optimum EDMing conditions on WC-6%Co. The issues are considered in the second part of this research.

Table 7. Finalized regression coefficients of the response models

Coefficient	MRR (g/h)	TWR (g/h)	Ra (μm)
β_0 (intercept)	0.2819	0.0454	4.8486
β_A	0.1937	0.0359	0.3019
β_B	-0.0631	-0.0116	0.8421
β_C	0.1096	0.0173	*Insignificant*
β_D	-0.0510	-0.0062	0.0759*
β_{A^2}	*Insignificant*	0.0119	*Insignificant*
β_{C^2}	-0.0139	-0.0071	*Insignificant*
β_{AB}	-0.0413	-0.0054	0.2143
β_{AC}	0.0755	0.0136	*Insignificant*
β_{AD}	-0.0423	-0.0051	0.2663
β_{BC}	-0.0168	-0.0046	*Insignificant*

*Note: The effect of gap voltage (D) on surface roughness is insignificant (see Table 5) and its coefficient has just been kept to comply with the *hierarchy* principle.

5. Conclusions

Based on the comprehensive model building attempts through the RSM, the following salient issues can be drawn:

I. All the main effects of input parameters, i.e., discharge current, pulse on-time, duty cycle, and gap voltage were found to be highly significant in affecting both the MRR and TWR. However, for the third response, the Ra, just the main effects of the first two factors (current and pulse on-time) were revealed to be statistically important.

II. The two way interaction effects of discharge current with pulse on-time (A×B), duty cycle (A×C), and gap voltage (A×D) as well as the interaction amongst the pulse on-time with duty cycle (B×C) and pure quadratic effect of duty cycle (C^2) have all been found to significantly control the MRR.

III. On the TWR measure, the same dual interaction effects influencing the MRR plus the pure quadratic effects of discharge current (A^2) were reached to be statistically significant. A more nonlinear behavior is then offered by the TWR.

IV. For the Ra response, the interactions between the discharge current with pulse on-time (A×B) and discharge current with gap voltage (A×D) possess significant effects.

V. The properly planed experimental layout through face-centered central composite design in conjunction with the response surface methodology provide immediate cognizance of the suitable combinations of operating parameters that may lead to optimum responses.

The procedure laid down can be generalized to develop a nomogram in a way that the suitable combinations of current setting, pulse on-time, duty cycle, and gap voltage for optimum material removal rate, tool wear rate, and surface finish can be easily determined altogether while EDMing such a selected WC-Co grade composite. This issue is of paramount concern for both EDM practitioners and academicians which will be studied in the second part of this research.

References

1 NorlianaMohd Abbas, Darius G. Solomon, Md. FuadBahari, A review on current research trend in electrical discharge machining (EDM), Int. J. Mach. Tools and Manufact., 47 (2007), 1214-1228.

2 K. H. Ho, S. T. Newman, State of the art electrical discharge machining (EDM), Int. J. Mach. Tools and Manufact., 43 (2003), 1287-1300.

3 P. Peças, E. Henriques, Intrinsic innovations of die sinking electrical discharge machining technology: estimation of its impact, Int. J. Adv. Manuf. Technol., 44 (2009) 880-889.

4 W. Konig, D. F. Dauw, G. Levy, EDM-future steps towards the machining of ceramics, Ann. CIRP, 37 (2) (1988), 623-631.

5 Thomas R. Newton, Shreyes N. Melkote, Thomas R. Watkins, Rosa M. Trejo, Laura Reister, Investigation of the effect of process parameters on the formation and characteristics of recast layer in wire-EDM of Inconel 718, Materials Science and Engineering, Part A, 513-514 (2009), 208-215.

6 Lin Gu, Lei Li, Wansheng Zhao, K. P. Rajurkar, Electrical discharge machining of Ti6Al4V with a bundled electrode, Int. J. Mach. Tools and Manufact., 53 (1) (2012), 100-106.

7 Yakup Yildiz, Murali M. Sundaram, Kamlakar P. Rajurkar, Optimization study and statistical analysis on the machinability of beryllium-copper (Be-Cu) alloy in EDM, ProcIMechE Part B: Journal of Engineering Manufacture, 226 (11) (2012), 1847-1861.

8 A. Dvivedi, P. Kumar, I. Singh, Experimental investigation and optimization in EDM of Al 6063 SiCP metal matrix composite, Int. J. Machining and Machinability of Materials, 3 (3/4) (2008), 293-308.

9 S. Gopalakannan, T. Senthilvelan, EDM of cast Al/SiC metal matrix nanocomposite by applying response surface method, Int. J. Adv. Manuf. Technol., DOI: 10.1007/s00170-012-4499-z. (Published online: 22 September 2012)

10 J. Luis, I. Puertas, Methodology for developing technological tables used in EDM processes of conductive ceramics, J. Mater. Process Technol., 189 (1-3) (2007), 301-309.

11 K. P. Rajurkar, G. Levy, A. Malshe, M. M. Sundaram, J. McGeough, X. Hu, R. Resnick, A. DeSilva, Micro and nano machining by electro-physical and chemical processes, Ann. CIRP, 55 (2) (2006), 643-666.
12 Kadirvel, P. Hariharan, S. Gowri, A review on various research trends in micro-EDM, Int. J. of Mechatronics and Manufacturing Systems, 5 (5/6) (2012), 361-384.
13 J. Paulo Davim, Machining of hard materials, Springer, 2011, ISBN: 978-1-84996-449-4.
14 J. B. J. W. Hegeman, J. Th. M. De Hosson, G. de With, Grinding of WC-Co hard metals, Wear, 248 (1-2) (2001), 187-196.
15 K. Liu, X. P. Li, Ductile cutting of tungsten carbide, J. Mater. Process Technol., 113 (2001), 348-354.
16 M. P. Jahan, M. Rahman, Y. S. Wong, A review on the conventional and micro-electro discharge machining of tungsten carbide, Int. J. Mach. Tools and Manufact., 51 (2011), 837-858.
17 R. Mahdavinejad, M. Mehraban, D. Mahdavinejad, The behavior of REFEL SiC under electro discharge machining, ProcIMechE Part B: Journal of Engineering Manufacture, 220 (10) (2006), 1635-1646.
18 R. K. Garg, K. K. Singh, AnishSachdeva, Vishal S. Sharma, KuldeepOjha, Sharanjit Singh, Review of research work in sinking EDM and WEDM on metal matrix composite materials, Int. J. Adv. Manuf. Technol., 50 (5-8) (2010), 611-624.
19 D. C. Montgomery, Design and analysis of experiments, 8th Edition, Wiley, New York, 2012, ISBN: 978-1-1183-9642-1.
20 R. H. Myers, D. C. Montgomery, CH. M. Anderson-Cook, Response surface methodology, 3rd Edition, Wiley, New York, 2009, ISBN: 978-0-470-17446-3.
21 D. C. Montgomery, E. A. Peck, G. G. Vining, Introduction to linear regression analysis, 5th Edition, Wiley Interscience, Hoboken, 2006, ISBN: 978-0-470-54281-1.
22 S. Assarzadeh, M. Ghoreishi, Statistical modeling and optimization of process parameters in electro-discharge machining of cobalt-bonded tungsten carbide composite (WC/6%Co), Procedia CIRP, 6 (2013), 464-469 (The 17th International Symposium on Electromachining (ISEM-XVII), April 9-12, 2013, Leuven, Belgium).